Symmetries, vibrational instabilities, and routes to stable structures of clusters of Al, Sn, and As

Raghani Pushpa,[a] Shobhana Narasimhan, and Umesh Waghmare
Theoretical Sciences Unit, Jawaharlal Nehru Centre for Advanced Scientific Research, Jakkur P.O. Bangalore 560 064, India

(Received 25 September 2003; accepted 14 June 2004)

We investigate the stability of small clusters using density functional theory to compute the total energy, forces, and vibrational frequencies using linear response. We exhibit an efficient and computationally low-cost route to finding stable structures, by starting with high-symmetry structures and distorting them according to their unstable modes. We illustrate this by application to 4-, 6-, and 13-atom clusters of Al, Sn, and As. This technique also naturally elucidates the origins of stability of the lower symmetry structures, which is variously due to the linear or pseudo Jahn-Teller effect, combined with a lowering of various contributions to the total energy. We show that the situation is more complex than has generally been appreciated. © *2004 American Institute of Physics.* [DOI: 10.1063/1.1779212]

I. INTRODUCTION

With the emerging importance of nanotechnology, the determination of the structure and properties of very small fragments of materials has become a pressing problem. While the structures of larger fragments can be understood as being derived from the bulk structures, this is not at all true for very small clusters, where the atomic arrangement can differ drastically from the bulk. However, determination of the structure of clusters is a very difficult problem, and in fact belongs to the computationally challenging category of Nondeterministic polynomial (NP) hard problems.[1] The problem is complicated by the fact that one often has nearly degenerate local minima, and one cannot be confident that one has in fact found the global minimum. Earlier authors have used various techniques, such as simulated annealing,[2] genetic algorithms,[3] etc. We have chosen to use a simpler route, which while being computationally undemanding (all our calculations have been performed on desktop single-processor PCs), gives answers that are in excellent agreement with previous, more sophisticated calculations. In some cases, we even get lower-energy structures than those known hitherto. Our approach consists of a loop that involves finding extremal structures by minimizing the Hellmann-Feynman forces, and systematically distorting the structures according to unstable vibrational modes that have been determined using density functional perturbation theory. This mimics the way in which the low-symmetry stable structures can be understood as being derived from high-symmetry structures via the Jahn-Teller coupling.

A related issue, to the discussion of which our approach naturally lends itself, is the interplay between the electronic structure and geometric structure of clusters. Upon examining the geometry of clusters, the first fact that one notices is that, almost always, the favored atomic arrangement is not one of high symmetry, though it can usually be obtained by a simple distortion of a high-symmetry structure. This has been noticed by previous workers in the field, and is usually attributed to the Jahn-Teller effect. However, the issue is not simple, and in this paper, we attempt to address some of the ramifications and subtleties involved. Changes in electronic configuration result in changes in the type of Jahn-Teller couplings that are allowed and/or dominate. In particular, we will distinguish between the linear and pseudo Jahn-Teller effects. Moreover, though the Jahn-Teller effect may be responsible for the instability of the high-symmetry structure, it does not always suffice to explain the particular low-symmetry structure that the cluster assumes. Instead, one has to look at the lowering of different contributions to the total energy (rather than simply the sum over the one-electron eigenvalues). We will investigate the relationship of symmetry and electronic structure of clusters with their structural stability, through the *ab initio* study of 4-, 6-, and 13-atom clusters of Al, Sn, and As. We investigate this issue in great detail through (i) group theoretical arguments, (ii) *ab initio* ''linear response'' calculations to determine the unstable vibrational modes of clusters with high-symmetry structures, (iii) ''frozen-phonon'' calculations with these unstable modes, (iv) an examination of changes in different contributions to total energy as the cluster is distorted from high-symmetry structures to the low-symmetry ones.

The reason we have chosen Al, Sn, and As is that they are all elements with only *s* and *p* electrons in their valence shells; however, the number of *p* electrons varies in the three cases. The electronic configuration in the outermost shell is Al, $3s^2 3p^1$; Sn, $5s^2 5p^2$; and As, $4s^2 4p^3$. The ordering of electronic levels is very similar in all three cases (in fact it is identical for Sn and As, and only very slightly different for Al); however, due to the addition of *p* electrons, the highest occupied molecular orbital (HOMO) and its symmetry are different in the three cases. This in turn modifies the Jahn-Teller mechanism in the three cases and we see diversity in the structural instabilities of these clusters and corresponding ground-state structures.

[a]Electronic mail: pushpa@jncasr.ac.in

Our work extracts the contributions of energy that are responsible for the relative stability of different low-energy atomic structures of these clusters, an accurate description of which is crucial for understanding their finite temperature properties. This could possibly guide the design of good interatomic potentials and tight-binding models that can be used in temperature-dependent simulations of the structural properties of clusters.

The structure of the paper is as follows. In Sec. II, we give an outline of our methodology and computational details. We obtain electronic energy levels using density-functional theory and vibrational frequencies using density functional perturbation theory (DFPT).[4] The interaction between these two leads to Jahn-Teller (JT) couplings; we discuss this in Sec. III, emphasizing the difference between different types of JT couplings. We then present, in Secs. IV, V, and VII, our results on 4-, 6-, and 13-atom clusters. For reasons of conciseness, a detailed symmetry analysis is presented only for the smaller clusters, and their origins of stability are discussed in Sec. VI. The section on 13-atom clusters is included to demonstrate that our approach works effectively even for larger cluster sizes with complex structures. We summarize and conclude in Sec. VIII.

II. METHODOLOGY

The determination of the low-energy or ground-state structures of larger clusters is a hard problem as the phase space for their exploration grows exponentially with the size of the cluster. This phase space can be partitioned into regions accessible from different high-symmetry structures, and the low-energy structures (often of low symmetry) can be derived as distorted forms of these high-symmetry structure. The eigenvectors of unstable vibrational modes of the high-symmetry structure provide precise pointers to the energy lowering structural distortions.

To determine stable, low-energy structures of clusters, we follow a loop, starting with a high-symmetry structure and (A) obtaining all its vibrational modes efficiently using density functional perturbation theory (DFPT), (B) identifying the unstable vibrational modes, (C) imposing displacements indicated by the eigenvectors of the strongest unstable mode and then relaxing the structure by minimizing the Hellmann-Feynman forces, (D) repeating (A), (B), and (C) until a structure with no unstable modes is obtained. The final structures are local minima of the energy, and a comparison of their energies yields the lowest-energy structure, which is a good candidate for the global minimum. The starting structure can either be a simple polygon or polyhedron (e.g., one of the platonic solids), or more complex polyhedra. Different initial choices (e.g., prisms versus antiprisms) frequently lead to the same final structure; though in some cases they lead to different structures that are nearly degenerate local minima of energy, and can be relevant to finite temperature properties of the clusters such as melting.

All our calculations were performed using *ab initio* density-functional theory calculations, using a plane-wave basis set and pseudopotentials. Recent advances in methodology have made this an approach that combines efficiency with reliability. Our calculations for total energy and forces were performed using the "PWSCF" package,[5] while vibrational modes were determined using DFPT as implemented in the "PHONON" package. Forces were obtained using the Hellmann-Feynman theorem, and ionic relaxation was carried out using the BFGS algorithm. A plane-wave basis cutoff of 20 Ry was used for all three elements, i.e., Al, Sn, and As. Exchange and correlation effects were described using the local density approximation (LDA).[6] While the use of the LDA may lead to an underestimation of bond lengths and a corresponding overestimation of cohesive energies, there are reports of opposite errors using other gradient-corrected functionals. However, these errors need not concern us here, as our interest is not so much in the absolute numbers as in obtaining the lowest-energy structures, and in idenifying the mechanisms and origins of structural instability. We expect these results to be fairly insensitive to the type of exchange-correlation potential used; also it has been reported that the LDA works better than the GGA for Sn.[7]

To check the quality/transferability of pseudopotentials, we first performed calculations on the bulk structures. For Sn in the diamond structure, we find that the lattice constant is 6.35 Å and the cohesive energy is 0.334 Ry/atom. For the β-Sn structure, the lattice constant a_0 is 5.70 Å and the cohesive energy is 0.338 Ry/atom. The experimental lattice constants are[8] 6.49 and 5.82 Å for the diamond and β-Sn structures, respectively. We verified that including or not including the $4d$ electrons as valence electrons does not make an appreciable difference to our results, and have therefore treated these electrons in the core. For bulk Al, we obtain the lattice constant and binding energy as 3.96 Å and 0.312 Ry/atom, respectively; the corresponding experimental values[8] are 4.05 Å and 0.249 Ry/atom.

For all cluster calculations, we use a unit cell (box) of dimension 24 bohrs with periodic boundary conditions. The dimensions of the box are large enough that the interaction between a cluster and its periodic images in neighboring boxes is negligible. We use just one k point, the Γ point (zone center) for Brillouin zone sampling. The total energy calculations were performed using thermal broadening to improve the convergence to self-consistency. For most of the results presented in this paper, we used Fermi-Dirac broadening with k_BT of 0.003 Ry, where k_B is the Boltzmann constant and T is the temperature.

As we use a large periodic unit cell to treat clusters, all vibrational modes are obtained through calculation of phonons at the Γ point $\vec{k}=(0,0,0)$ alone. Each case involves self-consistent calculation of first-order changes in Kohn-Sham wave functions (linear response) arising from perturbations corresponding to all symmetry independent atomic displacements. These wave functions are subsequently used in the determination of all the elements of the dynamical matrix, which is essentially the second derivative of total energy with respect to atomic displacements. Eigenvalues and eigenvectors of this matrix give the vibrational frequencies squared and mode eigenvectors, respectively. A negative eigenvalue of the dynamical matrix indicates a structural instability (or imaginary frequency) and the fact that energy is a maximum as a function of atomic displacements corresponding to its mode eigenvector. Note that our approach, of

using vibrational frequencies to minimize the energy, becomes feasible only with the advent of density functional perturbation (or 'linear response') theory, where all vibrational frequencies are simultaneously obtained while performing an *ab initio* calculation at a single structural configuration. The earlier approach of frozen phonon calculations would be prohibitively expensive if used for this purpose.

III. JAHN-TELLER COUPLING

The interaction of electronic states with nuclear motion is called the vibronic interaction[9] and has been studied extensively in molecules. It is particularly strong in some cases as discussed by Jahn and Teller, who showed that if the HOMO is degenerate and partially occupied, the molecule will always be unstable with respect to a distortion.[10] Hence it will distort from a high-symmetry structure to a lower symmetry structure lifting the degeneracy, thereby lowering the energy. This kind of vibronic coupling could occur in either linear or quadratic order in Q, the magnitude of the distortion away from the high-symmetry structure. For a system with linear JT coupling, a symmetry-breaking structural distortion results in the change in Hamiltonian that lifts the degeneracy at the HOMO. For example, if the HOMO is doubly degenerate, the electronic state of energy ϵ will split into $\epsilon \pm \langle \Delta V \rangle$, where ΔV is the perturbation potential and $\langle \cdot \rangle$ is the expectation value. For small distortions, $\Delta V \propto Q$ (with a positive proportionality constant). The energy of the HOMO is now lowered by ΔV and varies linearly with $|Q|$.

While the linear JT effect arises from the coupling of a single degenerate level with a symmetry-breaking structural distortion, the pseudo-JT effect arises from the mixing of an unoccupied state with an occupied state through a symmetry-breaking vibrational mode that is unstable (i.e., has imaginary frequency) in the high-symmetry structure. Upon distorting the system with this vibrational mode, the energy eigenvalue of a nondegenerate electronic state varies as

$$\epsilon_I = \epsilon_I^0 + \langle I|\Delta V|I\rangle + \sum_J \frac{\langle I|\Delta V|J\rangle\langle J|\Delta V|I\rangle}{\epsilon_I^0 - \epsilon_J^0}, \tag{1}$$

where $|I\rangle$ is the Ith electronic state of the high-symmetry structure with energy eigenvalue ϵ_I^0, ϵ_I is the energy of the Ith state after distortion (low-symmetry structure), and ΔV is the perturbation corresponding to this distortion. The second term on the right-hand side is zero for nondegenerate state I and ΔV with any irreducible representations other than the identity, as the right-hand side in the following vanishes,

$$\langle I|\Delta V|I\rangle \propto \sum_R \chi_I(R)\chi_I^*(R)\chi_{\Delta V}(R), \tag{2}$$

where R runs over the symmetry elements of the point group, and $\chi_I(R)$ and $\chi_{\Delta V}(R)$ are the characters of the irreducible representation corresponding to the electronic level I and the perturbation ΔV, respectively.

For $J > I$, the third term in Eq. (1) is negative and contributes to instability, but its overall contribution to the total energy is zero if I and J are both occupied. The pseudo-JT coupling between the Jth unoccupied and Ith occupied state thus lowers $\Sigma_I \epsilon_I$, which varies quadratically with the distortion Q, since $\Delta V \propto Q$.

For the pseudo-JT coupling to cause an instability (lowering of the *total* energy with distortion), the following condition has to be met:[9]

$$\Delta < |F_Q^{(1,2)}|^2 / K_Q^{(0)}, \tag{3}$$

where Q is the displacement of atoms from their high-symmetry positions, Δ is the gap $\epsilon_2 - \epsilon_1$ between the states 1 and 2, $F_Q^{(1,2)} = \langle 1|(\partial V/\partial Q)|2\rangle$, and $K_Q^{(0)} = \langle 1|(\partial^2 V/\partial Q^2)|1\rangle$. In general, K_Q is expanded to include the contribution of ion-ion interactions to the second derivative of the total energy with respect to Q.

Above, we have distinguished two kinds of JT effects. For a particular case, how does one determine whether a structural distortion is taking place due to the linear JT effect or the pseudo-JT effect? If there is no degeneracy in the HOMO, then the linear JT effect cannot occur, and any distortion must be due to the pseudo-JT effect. Otherwise, an examination of unstable modes combined with symmetry analysis can help distinguish between the linear and pseudo-JT effects. Perhaps the simplest way, however, is to look at curves of energy versus displacement (where the energy is computed for a series of snapshots of the system as one progresses from the high- to the low-symmetry structure). While the energy versus displacement shows a cusp at the high-symmetry structure ($Q=0$) for cases with a linear JT effect, for systems displaying a pseudo-JT effect the curve looks like a double well, with minima at the optimal low-symmetry structures and a maximum at the high-symmetry structure. Note that this implies that a system with pseudo-JT effect has imaginary vibrational frequencies for its high-symmetry structure.

However, the cusp in the energy function ($\epsilon = a|Q|$) at $Q=0$ in the case of systems with linear JT coupling strictly exists only at temperature $T=0$ K. Most calculations (and measurements) are performed with a nonzero temperature, which changes the nature of the energy function by smoothening the cusp. It can be readily shown that, upon occupying electronic levels according to the Fermi-Dirac distribution function for a finite temperature T, the expression for the energy ϵ takes the form,

$$\epsilon(Q,T) = -\frac{a^2Q^2}{2k_BT} + \frac{a^4Q^4}{24k_B^3T^3} - \cdots, \tag{4}$$

where a is the constant of linearity relating ϵ and $|Q|$ at zero temperature ($\epsilon = a|Q|$), and k_B is Boltzmann's constant. From this equation, it is clear that the free energy at finite temperature varies quadratically with displacement and has no cusp. As there are other contributions to energy at the quadratic order, the linear Jahn-Teller coupling may *not* give unstable modes in the vibrational spectrum, unless the inequality (3) is satisfied. At very low temperatures, however, the coefficients of Q^2 and Q^4 in Eq. (4) diverge, reflecting the cusplike nonanalytic nature of the energy surface.

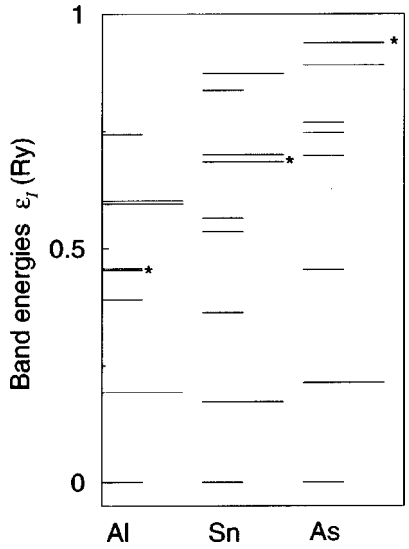

FIG. 1. Energy spectrum of four-atom square clusters of Al, Sn, and As. The ordering of energy levels is Al: A_{1g}, E_u, B_{2g}, B_{1g}, A_{2u}, A_{1g}; Sn: A_{1g}, E_u, B_{2g}, B_{1g}, A_{1g}, A_{2u}, E_u; As: A_{1g}, E_u, B_{2g}, B_{1g}, A_{1g}, A_{2u}, E_u, E_g. Levels marked by (*) are the HOMO levels. The length of the line segment represents the degeneracy of the level, short lines are nondegenerate, and long lines are doubly degenerate. Note that the HOMO for Al_4 is nondegenerate whereas for Sn_4 and As_4 it is doubly degenerate but of different symmetry.

IV. RESULTS: FOUR-ATOM CLUSTERS

There are two obvious high-symmetry structures for clusters composed of four atoms: the planar structure of a square, and the three-dimensional structure of a regular tetrahedron. We first consider these high-symmetry structures, optimizing the bond lengths. In most of the cases, the high-symmetry structure is not stable, as manifested by the presence of unstable vibrational modes upon performing linear response calculations on the structures of high symmetry. We then use these unstable modes as a guide to relaxing the structures and obtaining the low-symmetry stable structures.

We first consider square clusters and the low-symmetry structures derived from them. We find the equilibrium bond lengths for square clusters of Al, Sn, and As to be 2.58, 2.76, and 2.37 Å, respectively. We show in Fig. 1 the electronic spectra for these optimized square clusters. While the ordering of levels of different symmetry (indicated by the irreducible representation of the symmetry group D_{4h}) is very similar in all three cases, we note that the HOMO has a different symmetry in each of the three cases, due to the differing number of valence electrons. These results, along with the symmetry labels and frequencies of unstable modes, are summarized in Table I.

The stable structures were then determined by distorting the square with one or more of its unstable modes and relaxing the structure. The stabilization energy on going from D_{4h} to the stable structure is 0.017 Ry in Al, 0.112 Ry in Sn, and 0.061 Ry in As. Results for the symmetry properties of the HOMO and the unstable modes of these structures are summarized in Table II. It is clear that each of the three clusters exhibits a different behavior and we discuss the case of each element separately.

TABLE I. Results for the total energy E_{tot}, symmetry and degeneracy (deg) of the HOMO, symmetry of unstable modes, and their frequency ω for four-atom square shaped (D_{4h}) clusters with optimized size. The valence electron configuration for each element is also given.

Element	E_{tot} (Ry)	HOMO (deg)	Unstable modes	ω (cm^{-1})
Al ($3s^2 3p^1$)	−16.094	A_{2u} (1)	b_{2g}	86.1979*i*
Sn ($5s^2 5p^2$)	−28.032	E_u (2)	b_{2g}, b_{1u}	188.8789*i*, 128.6632*i*
As ($4s^2 4p^3$)	−50.633	E_g (2)	b_{1g}, b_{1u}	900.4501*i*, 217.0123*i*

As seen in Fig. 1, there is no degeneracy in the HOMO for the four-atom square Al cluster. This means that there can be no linear JT effect in this case. However, the pseudo Jahn-Teller effect, where an occupied and unoccupied state couple via an unstable mode, is possible. From group theoretic symmetry analysis, we find that the lowest unoccupied molecular orbital (LUMO), A_{1g}, can in principle couple with the occupied states B_{1g}, B_{2g}, and A_{2u}, through the vibrational modes b_{1g}, b_{2g}, and a_{2u}, respectively (Note: throughout this paper, we will use upper case letters for labeling the irreducible representations of electronic states and lower case letters for labeling the irreducible representations of vibrational modes). We can eliminate the a_{2u} mode as a possible instability since it corresponds to a translation of the whole cluster, and is therefore guaranteed to have zero frequency. Of the remaining two possibilities, b_{1g} and b_{2g}, our linear response calculations on square Al_4 show that only b_{2g} is unstable, i.e., the coupling is $(B_{2g} \oplus A_{1g}) \otimes b_{2g}$. This is somewhat surprising, given that B_{1g} is in fact closer to the LUMO than is B_{2g}, and one might therefore expect that b_{1g} should also be unstable. Upon distorting the square according to the b_{1g} mode, we find that the band energy (the sum over the energy eigenvalues of occupied states) increases, and therefore the condition for the pseudo-JT effect in Eq. (3) is not met.

The atomic displacement pattern corresponding to this b_{2g} mode (shown in Fig. 2) transforms the square cluster into a rhombus. We find that the stable structure of Al_4 is a rhombus with a bond angle of 64° and bond length of 2.52 Å. Two previous calculations also found that the optimal shape for the four-atom Al cluster is a rhombus. Petterson *et al.*, who used a many-body expansion of the Al-Al interaction potential, found the optimal bond length to be 2.66 Å, which is slightly larger than what we find, while an *ab initio* calculation by Jones[11] found results fairly similar to ours, with a bond length of 2.51 Å and an angle of 56° in the triplet state (which is the lowest in energy), and a parallelogram structure with bond lengths of 2.58 and 2.44 Å in the singlet state, which is slightly higher in energy than the triplet state.

Moving on now to tin, the HOMO of the Sn_4 square cluster has E_u symmetry and is a half-occupied doubly degenerate level. Symmetry analysis for the linear Jahn-Teller coupling yields two possible modes, b_{1g} and b_{2g}, which can lower the symmetry and energy of Sn_4. From linear response calculations of vibrational modes, we find that the unstable modes are b_{2g} and b_{1u}. Distorting the square Sn_4 with the b_{2g} mode lifts the degeneracy of the HOMO, splitting it into $\epsilon \pm \langle \Delta V_{b_{2g}} \rangle$, where $\langle \Delta V_{b_{2g}} \rangle = \langle E_u | b_{2g} | E_u \rangle$.

TABLE II. Results for total energy E_{tot}, freezing mode, symmetry of the HOMO, and degeneracy (deg), symmetry of unstable modes and their frequency ω after breaking the symmetry of the four-atom square cluster according to one or more of its unstable modes and allowing the structure to relax. The symmetry of the cluster is given in parentheses after the element name.

Element	E_{tot} (Ry)	Freezing mode	HOMO (deg)	Unstable modes	ω (cm^{-1})
Al (D_{2h})	−16.108	b_{2g}	B_{1u} (1)	⋯	⋯
Sn (D_{2h})	−28.140	b_{2g}	B_{3u} (1)	⋯	⋯
As (D_{2h})	−50.651	b_{1g}	B_{2g} (1)	b_{1u}	57.3723i
As (D_2)	−50.654	$b_{1g}+b_{1u}$	B_2 (1)	b_1	43.6709i
As (C_{2v})	−50.689	b_1+b_{1u}	B_1 (1)	⋯	⋯

As mentioned above, we also find that b_{1u} is unstable for the square Sn_4 cluster. Symmetry analysis reveals that this mode couples the HOMO E_u with the LUMO E_g, giving rise to the pseudo-JT effect. However, the b_{1u} instability is eliminated upon distorting the square cluster with the b_{2g} mode. Thus, b_{2g} and b_{1u} form a set of competing instabilities in the square Sn_4 cluster. The stable structure of Sn_4 has a rhombus shape in agreement with previous studies,[2,12] with bond lengths of 2.76 Å and bond angle 63°.

Finally, we consider the four-atom As cluster. The HOMO of the As_4 square cluster has E_g symmetry and is a partially occupied doubly degenerate level. Symmetry analysis for the linear Jahn-Teller coupling yields two possible modes, b_{1g} and b_{2g}, which can lower the symmetry and energy of As_4. From linear response phonon calculations, we find b_{1g} and b_{1u} modes to be unstable. Distorting square As_4 with the b_{1g} mode lifts the degeneracy at the HOMO and splits it into B_{2g} and B_{3g} (point group D_{2h}). Upon distorting the square according to b_{1g}, there is still an unstable mode b_{1u}.

We find from symmetry analysis that b_{1u} couples B_{3g} with B_{2u} giving a pseudo-JT effect. Distorting the square with b_{1g} and b_{1u} modes lowers the energy but there is an unstable eigenmode of symmetry b_{2g} (another pseudo-JT coupling). Finally, after further distorting according to b_{2g}, the system gets a puckered rhombus shape. The bond length and bond angles in the system are 2.35 Å, 66°, and 103°, respectively. This final structure of As_4 arises from the interplay between linear and pseudo JT effects.

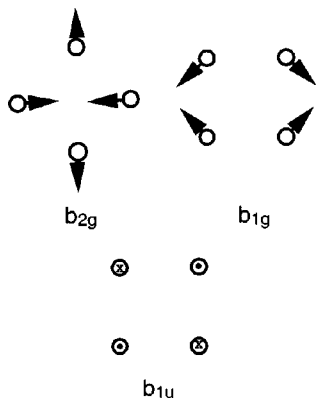

FIG. 2. Displacement pattern for four-atom square cluster in b_{2g}, b_{1g}, and b_{1u} mode.

Above, we explored structures of four-atom clusters which can be derived from a parent structure of square shape. Another high-symmetry structure that can be rather important in giving low-energy structures of four atoms is a tetrahedron, whose symmetry group is T_d. Starting with the initial structure as a regular tetrahedron and working through the same steps as we did for the clusters derived from the square one, we find that the rhombus structures we determined for Al_4 and Sn_4 are the lowest in energy. The rhombuslike structures of Al_4 and Sn_4 are, respectively, 0.024 and 0.102 Ry lower in energy than the structures obtained by working with a regular tetrahedron as the initial guess. In contrast, the undistorted (perfect) tetrahedron, which has a higher symmetry than that of a rhombus, has lower energy for As_4. It is 0.15 Ry lower in energy than the stable puckered rhombus structure, with the HOMO being degenerate but fully occupied, and there are no unstable modes. Partially, the reason for this high-symmetry structure being stable is that the HOMO is degenerate but fully occupied, so the linear JT effect is not possible in this system and the pseudo-JT effect is also excluded because of the large HOMO-LUMO gap of 0.313 Ry. The reason for having threefold coordination is that As has five valence electrons and if the bonding is covalent then three bonds will be formed to result in a completely filled (eight-electron) shell. This cannot happen for Al and Sn because we can have only one-, two- or threefold coordination in a four-atom cluster and there are three and four valence electrons in Al and Sn, respectively.

Therefore, for Sn_4, the perfect tetrahedron is 0.102 Ry higher in energy than the rhombus structure with no unstable modes. For Al_4 the perfect tetrahedron is 0.046 Ry higher in energy than the stable rhombus structure.

The lowest-energy structures for all three kinds of clusters are drawn in Fig. 3.

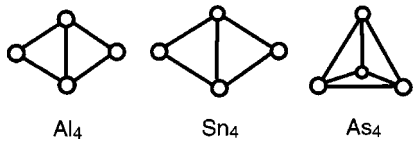

FIG. 3. The lowest-energy stable structures of four-atom clusters of Al, Sn, and As. Note that Al and Sn have low-symmetry structures whereas As has a high-symmetry structure as the stable structure.

TABLE III. Results for total energy E_{tot}, symmetry and degeneracy (deg) of the HOMO, symmetry of unstable modes, and their frequency ω for six-atom octahedral (O_h)-shaped cluster.

Element	E_{tot} (Ry)	HOMO (deg)	Unstable modes	ω (cm^{-1})
Al	−24.378	T_{2g} (3)	t_{2g}	260.6775i
Sn	−42.332	T_{1u} (3)	e_g	131.8468i
As	−76.001	T_{2u} (3)	$t_{2g}+e_g$	525.7227i, 131.8282i

V. SIX-ATOM CLUSTERS

One of the high-symmetry structures for six-atom clusters is that of a regular octahedron. None of the Al_6, Sn_6, and As_6 octahedral structures is stable; the vibrational spectrum of these clusters with equilibrium bond lengths (2.68, 2.93, and 2.59 Å, respectively) contain unstable modes, as reported in Table III. The electron energy spectrum for Al_6, Sn_6, and As_6 in the high-symmetry octahedral structure is shown in Fig. 4. The HOMO in all three cases is degenerate and the symmetry-allowed linear Jahn-Teller modes are e_g and t_{2g}.

The lower energy structures were then determined by distorting the octahedron with one or more of its unstable modes and relaxing the structure preserving its lower symmetry (a subgroup of O_h). The stabilization energy gained by distortion to a stable structure is 0.018 Ry for Al_6, 0.064 Ry for Sn_6, and 0.184 Ry for As_6. Results for the symmetry properties of the HOMO and the unstable modes of these structures are summarized in Table IV. Below, we discuss each case in detail.

For Al_6 clusters, we find that the HOMO is triply degenerate with symmetry T_{2g}. Symmetry analysis shows that two T_{2g} states can be coupled through a_{1g}, e_g, t_{1g}, t_{2g} modes making them potential modes of instabilities. Of these, a_{1g} corresponds to scaling of the structure and t_{1g} corresponds to rotation of the structure, hence a_{1g} has positive frequency and t_{1g} has zero frequency. The displacement patterns corresponding to the e_g and t_{2g} modes are shown in Fig. 5. From linear response calculations, we find that there is indeed a t_{2g} instability. After distorting the cluster with the t_{2g} mode and relaxing the structure maintaining its D_{2h} symmetry, there is still a b_{3g} unstable mode for this structure.

From compatibility relations between O_h and D_{2h}, we find that T_{2g} will be decomposed into A_g, B_{2g}, and B_{3g}. We find that A_g (HOMO) and B_{3g} (LUMO) couple with each other through b_{3g} giving rise to a pseudo-JT coupling, and an unstable b_{3g} mode. Thus, there are both linear and pseudo-JT effects active in the Al_6 cluster. Figures 6(a) and 6(b) show how the total energy varies as the cluster is distorted away from the regular octahedron, according to the mode t_{2g}. In Fig. 6(a), we see that the energy surface looks cusplike, as is characteristic of temperature $T=0$ K and the linear JT effect, whereas in Fig. 6(b), we see that at finite temperature, the energy function becomes smooth and quadratic for small distortions, and displays a double-well-like shape for larger distortions.

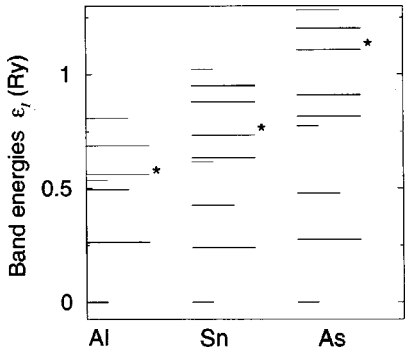

FIG. 4. Energy spectrum of six-atom octahedral clusters of Al, Sn, and As. The ordering of energy levels is Al: A_{1g}, T_{1u}, E_g, A_{1g}, T_{2g}; Sn: A_{1g}, T_{1u}, E_g, A_{1g}, T_{2g}, T_{1u}; As: A_{1g}, T_{1u}, E_g, A_{1g}, T_{2g}, T_{1u}, T_{2u}. Levels marked by (*) are the HOMO levels. Short, medium, and long lines are nondegenerate, doubly degenerate, and triply degenerate, respectively. Note that the ordering of energy levels in all three cases is the same but there are different HOMOs because the number of electrons in each system is different.

The structure of the Al_6 cluster, which has bond lengths of 2.53, 2.89, and 2.90 Å, is shown in Fig. 7, and has a lower symmetry than the trigonal antiprism structure with bond lengths of 2.51 and 2.86 Å, found by Jones.[11] In another previous calculation, Upton[13] found a D_2 structure as the lowest energy structure. Petterson *et al.*[14] studied the Al_6 cluster in structures of differing symmetry, and found that an octahedral structure has the lowest energy of all the structures studied by them. However, we find that the octahedral cluster has unstable modes, and breaking its O_h symmetry leads to a structure of even lower energy.

The triply degenerate and partially occupied HOMO of the octahedral Sn_6 cluster has T_{1u} symmetry, which allows a linear JT coupling for modes e_g and t_{2g}. Further, coupling the HOMO with the unoccupied T_{2u} level through these

TABLE IV. Results for the total energy E_{tot}, freezing mode, symmetry and degeneracy (deg) of the HOMO, symmetry of unstable modes and their frequency ω after breaking the symmetry of the six-atom octahedral cluster according to one or more of its unstable modes, and allowing the structure to relax. The symmetry of the cluster is given in parentheses after the element name.

Element	E_{tot} (Ry)	Freezing mode	HOMO (deg)	Unstable modes	Frequency (cm^{-1})
Al (D_{2h})	−24.379	t_{2g}	A_g (1)	b_{3g}	296.6624i
Al (C_{2h})	−24.397	$t_{2g}+b_{3g}$	A_g (1)	⋯	⋯
Sn (D_{4h})	−42.396	e_g	E_u (2)	⋯	⋯
As (D_{2h})	−76.112	t_{2g}	A_u (1)	b_{3g}	107.7205i
As (C_{2h})	−76.121	$t_{2g}+b_{3g}$	A_u (1)	b_g	213.2122i
As (C_i)	−76.184	$t_{2g}+b_{3g}+b_g$	A_u (1)	⋯	⋯

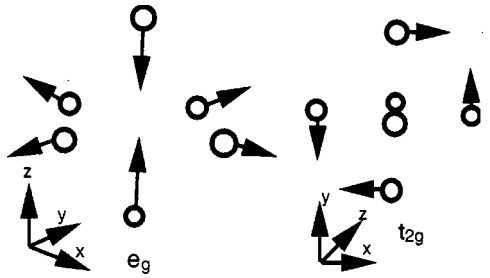

FIG. 5. Displacement patterns for six-atom octahedral cluster in e_g and t_{2g} modes. For convenience, different views are used for the two modes. In e_g there is expansion of the square in the xy plane wheareas atoms come closer together along z. In t_{2g} atoms in the xy plane form a rectangle whereas atoms along z direction are stationary.

modes can also yield a pseudo-JT effect. Of these possible instabilities, only e_g is found to be unstable in our calculations of the vibrational spectrum (see Table III). The e_g mode corresponds to ''squashing'' of the octahedron, as depicted in Fig. 5.

Distorting the octahedral cluster according to the e_g mode lowers the symmetry to D_{4h}, and also lifts the degeneracy of the HOMO. The calculated vibrational spectrum of this distorted cluster shows no unstable modes, implying that there is only one active mode in this system which gives both the linear and pseudo JT couplings in the system. The stable structure for this cluster has the D_{4h} point group with two intersecting rhombi, in agreement with the results of previous studies,[2,12] where Lu *et al.* do Car-Parrinello molecular dynamics simulated annealing on these clusters and find two degenerate structures, of which one consists of intersecting rhombi.

The octahedral As_6 cluster has a partially occupied and triply degenerate HOMO of T_{2u} symmetry (which implies that both e_g and t_{2g} can be linear JT active). The coupling of the HOMO with the occupied T_{1u} state makes these modes pseudo-JT active as well. Our calculations of the vibrational spectrum of the octahedral As_6 cluster show that both the e_g and t_{2g} modes are indeed unstable (see Table III), confirming the predictions of symmetry analysis.

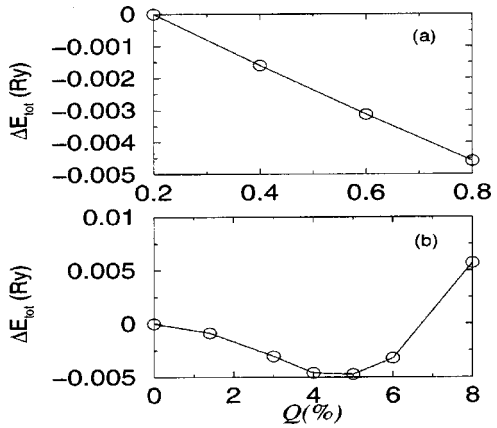

FIG. 6. For Al_6, total energy vs Q (displacement of atoms from their high-symmetry positions). (a) No thermal broadening is used, and the curve is linear, (b) a thermal broadening of 0.003 Ry is used and the curve now looks quadratic for small Q, and like a double well for larger Q.

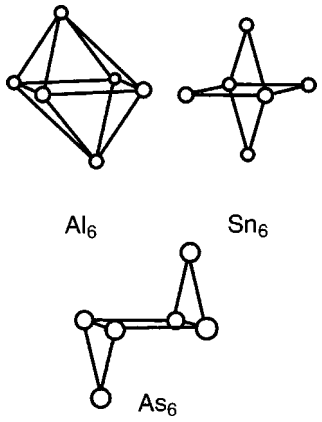

FIG. 7. The lowest-energy structures of six-atom clusters of Al, Sn, and As.

Using compatibility relations, we find that T_{2u} decomposes into A_u, B_{2u}, and B_{3u} states as the cluster is distorted according to the t_{2g} mode, lowering its symmetry to D_{2h}. The resulting cluster shows yet another instability: mode b_{3g}; we find that A_u and B_{3u} states couple with each other through the b_{3g} vibrational mode giving rise to the pseudo-JT effect. A further distortion of this structure according to the b_{3g} mode has C_{2h} point group of symmetry, and has the unstable mode b_g, which arises from pseudo-JT coupling between the A_u and B_u states. The final structure has only inversion symmetry.

The lowest-energy structures for all three kinds of six-atom clusters are drawn in Fig. 7.

VI. ENERGY CONTRIBUTIONS TO THE STABILITY OF FOUR- AND SIX-ATOM CLUSTERS

While the Jahn-Teller arguments might explain why the high-symmetry structures are not stable, they do not necessarily suffice to explain why the system assumes a particular low-symmetry structure that minimizes the total energy. For this we examine the change of different contributions to the total energy upon distortion of the system. We can separate out different contributions to the total energy as, $T+E_{xc}+E_{es}+E_{th}$. Here T is the kinetic energy, E_{xc} is the exchange-correlation energy, E_{es} is the electrostatic energy having contributions from Ewald (E_{ew}), electron-ion (E_{ei}), and Hartree (E_H) energies. E_{th} is the correction due to thermal broadening. Kinetic energy and exchange-correlation energy are purely quantum mechanical contributions, whereas the electrostatic term is classical.

For Al_4 and Sn_4, we find that both the classical and quantum mechanical terms are responsible for lowering of the energy. In contrast, for As_4, only the quantum mechanical terms are responsible for the same. For Al_6 the exchange-correlation and electrostatic energy are responsible for the stabilization of structure. One's intuition would say that if there is a JT effect, then the bandsum (sum over occupied electronic levels, $\Sigma_I \epsilon_I$) should decrease as we go from the high- to the low-symmetry structure. Surprisingly, we find that for Al_6, this bandsum increases upon distortion from the high-symmetry structure that minimizes the total energy. However, upon closer examination, we find that at very small

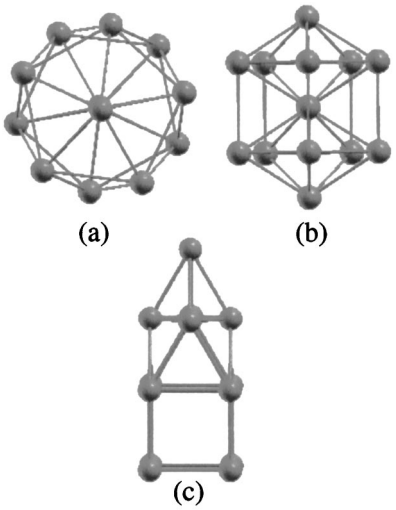

FIG. 8. Different high symmetry structures of a 13-atom cluster. (a) Regular icosahedron, (b) modified icosahedron, (c) structure with C_{4v} symmetry.

distortions, the bandsum does decrease, i.e., the instability in the system is initially driven by JT coupling, but as the distortion increases, other effects start dominating and drive the system to the particular lower-symmetry structure that is finally favored. For Sn_6, all the three interactions (electrostatic, exchange correlation, and kinetic energy) contribute to the stability of the system. Finally, for As_6, while both linear and pseudo JT effects drive the instability of the octahedral structure, the ground state is stabilized mainly due to the electrostatic and electronic kinetic energies.

VII. LOW-ENERGY STRUCTURES OF 13-ATOM CLUSTERS

In previous sections, we have used our approach to determine the structures of four- and six-atom clusters. However, to exhibit the power and efficacy of our method, we now apply the same approach to the nontrivial problem of finding the structures of 13-atom clusters.

We consider here three high-symmetry starting structures (see Fig. 8): (a) a regular icosahedron with symmetry group I, (b) a modified icosahedron with a horizontal mirror plane symmetry and symmetry group D_{5h}, and (c) a structure with a fourfold rotational symmetry C_{4v} obtained by placing a square and a capping atom on top of a cubic structure. While the structure (a) is a Platonic one, (b) and (c) have been designed just to have certain symmetries.

For Al_{13} the icosahedral structure (a) has no unstable vibrations, but can be relaxed, yielding a distorted structure with energy -53.466 Ry. The structure (b) is found to be unstable and leads to a final locally stable structure (energy $E=-53.467$ Ry, an energy lowering of 0.03 Ry relative to the starting structure), through an intermediate unstable structure. The structure (c) is also found to be unstable and leads to a final locally stable structure ($E=-53.305$ Ry) with an intermediate unstable structure. A careful examination of final structures shows that the fully relaxed structures derived from (a) and (b) are essentially the same. Note that though the symmetry and bonding topology are different in

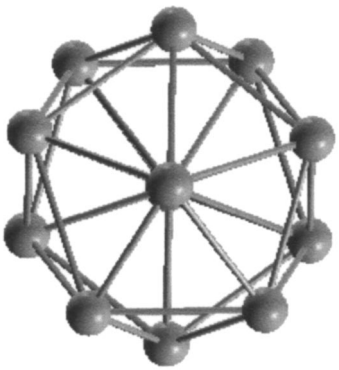

FIG. 9. The lowest-energy stable structures of Al_{13} clusters.

(a) and (b), the two can be related to each other by a rotation of a pentagon by 72°. The lowest-energy structure, shown in Fig. 9, agrees with that reported in Ref. 15.

For Sn_{13}, we find the icosahedral structure stable with an energy of -91.975 Ry. The structure (b) has five unstable modes and when relaxed with respect to the strongest instability results in another structure that is unstable, again with five unstable modes. This structure, when relaxed further, results in a locally stable structure (see Fig. 10) with energy -92.033 Ry (overall energy lowering of 0.1 Ry). When the structure (c) was relaxed through two iterations of this approach, we find the final structure with energy of -92.086 Ry, lowest in energy. For comparison with earlier work, we also started with the initial structure reported in Ref. 12 and relaxed it within our calculational procedure (see Fig. 10 for both the structures). We found its energy to be -92.059 Ry, about 0.027 Ry higher than our lowest energy structure. Thus, our relatively simple approach is sometimes able to find structures that are lower in energy than those obtained

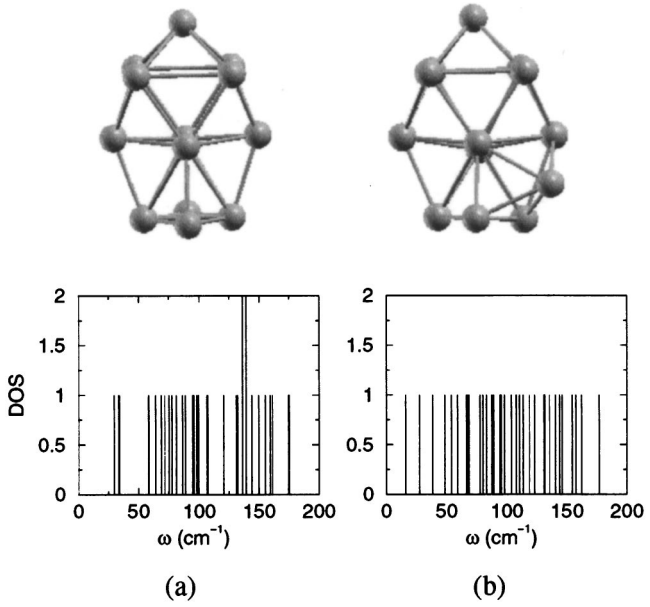

FIG. 10. The lowest-energy stable structures of Sn_{13} clusters and the corresponding vibrational spectrum (a) derived from high symmetry structure with point group C_{4v} [shown in Fig. 8(c)], (b) structure obtained by Majumder *et al.*

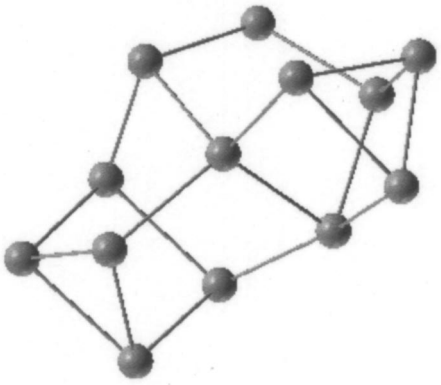

FIG. 11. The lowest-energy stable structures of As_{13} clusters.

previously using more sophisticated and expensive methods. To resolve the question of the structure of the lowest energy and aid further experimental studies, we have included our calculated vibrational spectra of these locally stable structures in Fig. 10.

In the case of As_{13} clusters, we first start with the regular icosahedron and relax the structure. The resulting structure has an energy of -164.973 Ry and lower symmetry than that of the regular icosahedron. While it has five unstable modes, its energy is 0.18 Ry higher than the initial icosahedral structure (b), hence we did not relax it further using these unstable modes. The icosahedral structure (b) was found to have only one unstable mode, and two iterations of the present approach with this as a starting point result in the final stable structure at an energy of -165.257 Ry (an overall energy lowering of 0.107 Ry). Looking at the valency of As, one would expect As_{13} not to be very stable, but indeed the energy per atom of this final structure (shown in Fig. 11) is lower than that of As_4 and As_6. The origin of its stability can be seen in the structure which has ten atoms with coordination number (CN) of 3, two with CN of 2, and one with CN of 4.

VIII. SUMMARY AND CONCLUSIONS

We have performed *ab initio* density-functional theory calculations and *ab initio* linear response calculations to calculate the total energy and vibrational modes of 4-, 6-, and 13-atom clusters of Al, Sn, and As. We have confirmed some previous results for Al and Sn clusters, and have in fact found a lower energy structure for Sn_{13} than that previously reported. We are not aware of any previous results on As clusters of these sizes.

In this paper, the low-energy structures of clusters were determined by a systematic examination of unstable modes obtained using *ab initio* linear response calculations. Our way of progressing from high-symmetry to low-symmetry structures via vibrational instabilities is conceptually simple, computationally efficient, and has the additional advantage that it mimics the actual way in which the JT effect leads to particular low-symmetry structures. A combined examination of electronic and vibrational structure enables one to guess what the final structure might be. We do note, however, that our method does require that one repeats the procedure with a variety of starting structures of high symmetry (e.g., the square and the tetrahedron for the four-atom case) to ensure that one has found the true ground-state minimum.

While the role of the JT effects in determining cluster structures is well known, we emphasize the subtle difference between the linear and pseudo JT effects, and have illustrated that, depending on the electronic structure, one may have either or both, resulting in different final structures. Thus, for four-atom clusters, for Al there is a pseudo-JT effect only, for Sn the linear and pseudo JT effects compete, with the former ''winning,'' while for the As structure derived from the square, both types of effects contribute, and for that derived from the tetrahedron, neither contributes.

For the six-atom clusters, in all cases, we find that both the linear and the pseudo JT effects are responsible for lowering the symmetry of the structure, but the way in which these effects operate is different in each case. For Al, there are two unstable modes, one resulting from the linear JT effect and the other from the pseudo-JT effect; for Sn, there is a single unstable mode, which contains both kinds of JT effects, and for As, there are two unstable modes, both of which contain both kinds of JT effects.

So, while it is indeed true that high-symmetry structures are disfavored due to the Jahn-Teller effect, the actual situation is quite complex, with the details of the picture changing in each case due to the differing electronic configuration of the elements.

Moreover, the two kinds of Jahn-Teller effects alone do not suffice to tell the whole story. In other words, it is not enough to look at just the band sum (sum over occupied electronic energy eigenstates) but one must also look at the various classical and quantum mechanical contributions to the total energy of the system. The relative contributions of these different terms change as one changes the atomic species and/or the number of atoms in the cluster. This complicated scenario explains, in part, why it has proved so difficult to develop a reliable interatomic potential for the accurate energetics of clusters of different sizes.

ACKNOWLEDGMENTS

We acknowledge helpful discussions with Rajendra Prasad, Vijay Kumar, and Chiranjib Majumder. S.N. acknowledges the Associateship program of the Abdus Salam International Center for Theoretical Physics, as well as the Chemistry Department of the University of Cambridge, where a part of this paper was written. All the calculations were carried out on the central computing facilities at JNCASR, supported by the Department of Science and Technology of the Government of India.

[1] L. T. Wille and J. Vennik, Chem. Rev. (Washington, D.C.) **18**, L419 (1985).
[2] Z. Y. Lu, C. Z. Wang, and K. M. Ho, Phys. Rev. B **61**, 2329 (2000).
[3] K. M. Ho, A. A. Shvartsburg, B. Pan, Z. Y. Lu, C. Z. Wang, J. G. Wacker, J. L. Fye, and M. F. Jarrold, Nature (London) **392**, 582 (1998).
[4] S. Baroni, P. Giannozzi, and A. Testa, Phys. Rev. Lett. **58**, 1861 (1987).
[5] S. Baroni, A. Dal Corso, S. de Gironcoli, and P. Giannozzi, http://www.pwscf.org
[6] J. P. Perdew and A. Zunger, Phys. Rev. B **23**, 5048 (1981).

[7] A. Aguado, Phys. Rev. B **67**, 212104 (2003).
[8] C. Kittel, *Introduction to Solid State Physics*, 5th ed. (Wiley, New York, 1976).
[9] I. B. Bersuker, Chem. Rev. (Washington, D.C.) **101**, 1067 (2001).
[10] H. A. Jahn and E. Teller, Proc. Roy. Soc. A **161**, 220 (1937).
[11] R. O. Jones, J. Chem. Phys. **99**, 1194 (1993).
[12] C. Majumder, V. Kumar, H. Mizuseki, and Y. Kawazoe, Phys. Rev. B **64**, 233405 (2001).
[13] T. H. Upton, J. Chem. Phys. **86**, 7054 (1987).
[14] L. G. M. Pettersson, C. W. Bauschlicher, and T. Halicioglu, J. Chem. Phys. **87**, 2205 (1987).
[15] V. Kumar, S. Bhattacharjee, and Y. Kawazoe, Phys. Rev. B **61**, 8541 (2000).